Surface phase stability diagram for Pd deposits on Ni(110): A first-principles theoretical study

J.-S. Filhol, D. Simon, and P. Sautet
Laboratoire de Chimie Théorique et des Matériaux Hybrides, École Normale Supérieure de Lyon, 46 Allée d'Italie, 69364 Lyon Cedex 07, France
and Institut de Recherches sur la Catalyse, CNRS, 2 avenue A. Einstein, 69626 Villeurbanne Cedex, France
(Received 23 February 2001; published 7 August 2001)

Different surface structures of Pd deposits on Ni(110), from alloys to ordered phases, in a range between 0.125 monolayer and near 4 monolayers, have been studied using density functional calculations. The main feature of these deposits is the stress exerted by the Ni substrate on the Pd atoms, due to the size difference between the two metals. The surface phase stability diagram has been constructed, allowing to find the most stable surface structures at a given coverage. At low coverage ($\leqslant 0.7$ monolayer), the disordered alloy phase is found to be stable. Then, at higher coverage, ordered surface structures are stable, and a mixing of some of them can coexist in some ranges. Between 0.7 and 1 monolayer, the surface presents an equilibrium between the alloy phase (containing 70% of Pd atoms) and a 1 monolayer phase. In the 1–4 monolayers range, the equilibrium is set up between the two extreme phases: 1 monolayer and 4 monolayers: These deposits show a peculiar structure, in which a periodical Pd vacancy at the Ni-Pd interface ensures the release of the stress and induces a heteroepitaxial dislocation. The stability of these structures versus the coverage is discussed as a competition between surface alloying and surface stress. Finally, the electronic structure of these phases is studied and appears to be closely linked to the surface strain of the Pd deposit, even for the alloy phases. These bimetallic surfaces reveal a wide range of local density of states, simply by changing the Pd coverage. Then, the possibility to tune the specific catalytic properties of these deposits is discussed.

DOI: 10.1103/PhysRevB.64.085412 PACS number(s): 68.35.Bs, 68.35.Md, 73.20.At

I. INTRODUCTION

Bimetallic surfaces have already been widely investigated.[1] However, there still is a great deal of interest for these compounds that show many particular properties and interesting behaviors from catalysis to information storage. The reactivity of metal catalysts, for example, can be modified by depositing the active metal on another metallic substrate, with different geometric or electronic properties. In particular, deposits of Pd on Ni(110) have shown an enhancement of the catalytic activity for the partial hydrogenation of butadiene, with an increase of two orders of magnitude for moderately annealed four-layer thick systems compared to the pure Ni or Pd surfaces.[2–6] Moreover, the excellent selectivity of Pd for the hydrogenation of a single insaturation of the two double-bond butadiene molecule is kept.

A key point for the deposits is the difference in size between the two metals. In the case the of Pd on Ni(110), the misfit is close to 10%, the bulk diameter of Pd (2.75 Å) being larger than that of Ni (2.49 Å). Low-energy electron diffraction, (LEED) scanneling tunneling microscopy (STM) and x-ray diffraction have shown that the deposit of Pd on Ni(110) is not pseudoepitaxial, but that the compressive stress in the layers is released by the formation of complex reconstructions, which depend on the Pd coverage.[7,8] A different behavior is observed in the two inequivalent directions of the Ni(110) substrate, with a long periodicity (6 to 11 times that of the Ni substrate as a function of Pd coverage) in the direction along the close-packed [110] rows, and a simple or double periodicity perpendicular to the rows ([100] direction). The complexity of these deposits and the dependence of the surface reconstruction with the coverage, make the complete experimental determination of the surface structures difficult. These deposits are characterized by a certain polymorphism and several types of domains can compete on the surface. The potential coexistence of phases makes the experimental or theoretical analysis of the structure even more difficult. However, the detailed understanding of the catalytic reactivity of these deposits requires a precise knowledge of the stable surface structures as a function of Pd coverage. The simple hard sphere model that was used previously[8] cannot be directly applied to these systems, due to the important geometric misfit between Pd and Ni, and more precise simulation techniques need to be involved. Metal alloys and deposits have already been the subject of several theoretical studies.[9–15]

Surface stress and alloy effects are the factors that have been pushed forward in order to explain the change in electronic structure and chemical reactivity. Models for the quantum calculations are simple pseudoepitaxic systems. However, the relaxation of the stress in these deposits can create, as seen from the experiments, new surface structures with unusual atomic coordinations, which in turn could be a key explanation for the specific reactivity. Hence a systematic analysis of the energy and structure of the various phases as a function of coverage can give important insights in the respective role of residual stress or specific atomic structure for the catalytic activity of these deposits. This is our aim in this paper for the case of deposits of Pd on Ni(110) and in a range of coverage between 0 and 4 monolayers (ML). After a brief description of the calculation method (Sec. II), the optimal structures are presented in Sec. III. The associated energies are then gathered in a surface phase stability diagram (Sec. IV). The obtained structures with various sizes of re-

construction will be associated with their electronic properties, in relation with their potential reactivity (Sec. V).

II. CALCULATION METHOD AND COMPUTATIONAL CONDITIONS

Pd-Ni surfaces are represented by periodic slabs. These slabs are repeated in a super-cell geometry with at least 8 Å of vacuum between them. The Ni substrate is made of 5 layers. The repetition vector in the $[1\bar{1}0]$ direction is $\Lambda d_{\text{Ni-Ni(Bulk)}}$, where $\Lambda = 1-11$ and $d_{\text{Ni-Ni(Bulk)}}$ is the Ni-Ni distance in the bulk. The calculations were performed using the plane-wave density-functional code VASP[16,17] with Vanderbilt ultrasoft pseudopotentials[18,19] for both Pd and Ni. The exchange-correlation energy and potential are described by the generalized gradient approximation [Perdew-Wang 91 (Ref. 20)]. The comparison of systems with large variations of the cell parameters imposes a high accuracy in the *k*-space integration. A Monkhorst-Pack mesh of $18\times9\times1$ was used for $\Lambda = 1$ and the *k*-point sampling density in the reciprocal space was maintained as constant as possible with the size increase of the supercell at least for the $\Lambda\times1$ structures. For the 11×2 structures (corresponding to a Pd deposit around 4 ML), a Monkhorst-Pack mesh of $1\times3\times1$ was used: the *k*-point sampling density is then lower, due to the size of these systems that are composed with 190 atoms. However, the geometric structure is still converged with these conditions and the energy allows comparisons with other related systems with an accuracy of 25 meV/Pd atom, which is considered as sufficient for our purpose.

The structures that we have investigated are mainly induced by the stress that arises from the difference in size between the Ni substrate and the Pd absorbate. However, in our calculations, the optimized Pd bulk diameter happens to be a little larger (2.80 Å in bulk calculation) than in reality (2.75 Å). This is mainly due to the approximated exchange-correlation functional used in the DFT approach. Hence, as the bulk calculated Ni-Ni distance is the same as experimentally (2.496 Å versus 2.491 Å, respectively), the epitaxial stress to which the Pd atoms are submitted, is slightly stronger in the calculated than in the true surface. As we shall see, a defect in the surface structures is assumed to allow the stress release inducing periodical structures. Consequently, as more stress should induce more defects, we expect that the calculated periodical reconstructions are characterized by a frequency of defects slightly larger than what can be found experimentally.

III. Pd/Ni(110) SURFACE STRUCTURES

The calculated structures for the deposits of Pd on Ni(110) will be presented in this section, starting from low coverage structures [1 monolayer (ML) and less] and going to thicker layers up to 4 ML.

A. Low-coverage structures

1. The epitaxial deposit

The perfect epitaxial monolayer of Pd/Ni(110) is used as an energy reference for the Pd adsorption energy. It corresponds to a 1 monolayer coverage. The choice of a two-dimensional (2D) growth for this deposit is justified by the calculation of the adsorption energy of a Pd atom on Ni(110), as compared to the energy of a Pd atom in Pd bulk. The former is 220 meV more stable than the latter, so the formation of islands of bulklike Pd is not favored and the growth occurs in a Franck–van der Merwe mode.

This structure is obviously highly stressed since the Pd atoms are submitted to the Ni parameter, 2.49 Å. The stress is compressive, and we have shown in a previous work[9] that it could be relaxed in an ideal way by increasing the Pd-Pd distance to 2.72 Å. The energy associated with this stress relaxation has been estimated to 90 meV by Pd atom. Therefore, the epitaxial deposit is certainly unstable and should undergo a reconstruction to minimize the energy of the system. Two possible ways to relax this kind of surface have been investigated. The first one is the formation of a surface alloy, and the second is the development of periodic vacancies.

2. Surface alloy

As a solid solution is obtained at any composition in a bulk Pd-Ni alloy, the formation of a surface alloy can be expected from a Pd deposit on Ni(110). We have studied surface Pd-Ni alloys formed from Pd deposits associated with various coverage between 0.1 monolayer and 1 monolayer. This allows us to calculate the formation energy of an alloyed surface layer with a composition ranging from a diluted Pd solution to an epitaxial Pd monolayer. Because of the use of a periodical DFT code, we can only study ordered alloys [Fig. 1(a)], but, by using large cells with low symmetry, the case of unordered surface alloys can be approached. In order to compare the energy of the surface alloys of different compositions, we calculate the energy associated with an equilibrium between a purely epitaxial Pd/Ni(110), surrounded by a naked Ni(110) surface, and the alloyed surface. Figure 1(b) depicts the energy, by Pd atom, for this equilibrium, versus the Pd coverage. First, at low coverage (0.1–0.3 monolayer), the alloy is very stable, with a stability of nearly 150 meV by Pd atom, as compared to the epitaxial surface. For a higher coverage, the energy by Pd atom increases, but the surface alloy remains more stable than the epitaxial structure in any case.

At this point, in order to study the ordering of these alloy phases, it is important to test the variation of the energy with the distance between the Pd atoms in the alloy configuration. We can calculate the evolution of the energy of a given slab containing two Pd atoms, when the relative position of these two Pd atoms is changed in the elementary cell. For example, in a 8×1 cell with 2 Pd atoms, the system with two neighboring Pd atoms is only destabilized by 30 meV compared to a cell with Pd atoms at a distance of 10 Å. Then, at a given coverage the energy change of different configurations of the alloy is estimated to a few tenth of meV, only.

The low-coverage calculations have shown that alloying, which tends to create Pd-Ni bonds, seems to be very favored. This contrasts with the fact, just shown above, that the relative position of Pd atoms in the surface, and hence the number of Pd-Ni bonds, does not significantly change the energy.

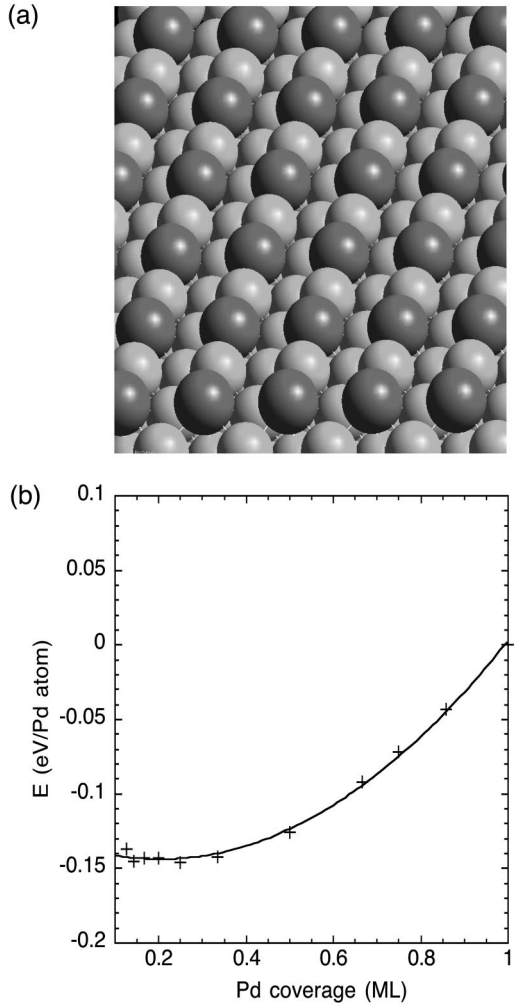

FIG. 1. Surface alloy for Pd on Ni(110). (a) Surface view of an ordered configuration for a Pd coverage of 0.5 ML. The Pd atom is indicated by a dark ball, while the Ni atom is shown as a smaller light ball. (b) Energy (eV per Pd atom) vs Pd coverage. The limiting structure for a coverage of 1 ML is the epitaxial deposit, and it is the energy reference.

So, something must counteract the creation of Pd-Ni bonds to explain this small energy dependence of the relative Pd position. A good candidate is the stress release linked with the difference of size between Pd and Ni. This phenomenon can be demonstrated on the example of a 4×1 alloy cell with two Pd atoms by comparison of the two following sequences: the alternating sequence Pd-Ni-Pd-Ni and the paired sequence Pd-Pd-Ni-Ni. The energy difference between these two cells is small (around 25 meV) as found previously for the larger 8×1 cell. The alternating sequence is constrained by symmetry, having all its surfaces atoms on epitaxial sites: it cannot release the stress. However, there are four surface Pd-Ni bonds by unit cell. In contrast, the paired sequence cell has only two surface Pd-Ni bonds but the surface atom can laterally relax to partially decrease the stress: the Pd-Pd distance increases to 2.66 Å, and the Ni-Ni distance decreases to 2.36 Å.

In order to detail the influence of relaxation on the surface energy, we have then calculated the energy of a paired sequence, but with all the surface atoms maintained in their epitaxial sites. In a first approximation, this allows us to estimate the creation enthalpy of two Pd-Ni bonds (starting from a Pd-Pd and a Ni-Ni bonds), at a frozen geometry: we find a value of 145 meV. Additionaly, the stress energy release for the two Pd of the relaxed paired sequence can be estimated to 120 meV, which leads to the small energy difference (of only 25 meV) between these two configurations.

TABLE I. Evolution of the Pd-Pd distance in a Pd_2 pair embedded in a Pd-Ni alloy surface, as a function of the composition of the surface.

Surface Pd Ratio	Pd-Pd distance (Å)
0.25	2.68
0.50	2.66
0.66	2.62
0.75	2.58
0.86	2.54
1.00	2.50

We can hence clearly see that the weak mixing enthalpy between Pd and Ni in these surface alloys is directly linked to the near cancellation between the Pd-Ni bond formation energy (which favors the mixing) and the surface stress release (which favors the segregation) in Pd islands with larger distance between Pd atoms and Ni islands with shorter Ni-Ni distances (the surface atoms tend to be under tensile stress[21,22]).

Furthermore, at a temperature of 600 K, which is the annealing temperature for these systems, the mixing entropy of a disordered surface alloy gives a typical stabilization of 70 meV by Pd atom. Then, the free energy gain associated with the mixing entropy at a coverage of 0.25 ML is larger than the loss of enthalpy linked with the access of less stable configurations with closer Pd atoms. Hence, we expect a disordered surface alloy.

If the alloy is stable at low coverage, it is rapidly destabilized when reaching the 1 ML situation. In the dilute case, the particular stability from the alloy structure can be associated, on one hand, with the creation of Pd-Ni bonds that appear to be energetically favored, and on the another hand, with the fact that nearly all the Pd stress can be released in many surface Ni atoms that elastically absorb this stress. Two effects concur to destabilize the alloy at a coverage larger than 0.5 ML. First, the average number of Pd-Ni bonds decreases with the coverage. Second, the release of the compressive stress for the Pd atom is reduced. This can be illustrated from the variation of the Pd-Pd distance in a surface pair, when the Pd coverage is changed. Compared to the epitaxial situation, the Pd-Pd distance is strongly increased in low Pd coverage alloys, while the stress realeased is rapidly hindered for higher coverages (Table I).

3. Vacancy structure

In a previous Letter, we have studied the case of periodical vacancy formation in the deposit.[9] This family of structures is obtained from the 1 ML epitaxial situation by remov-

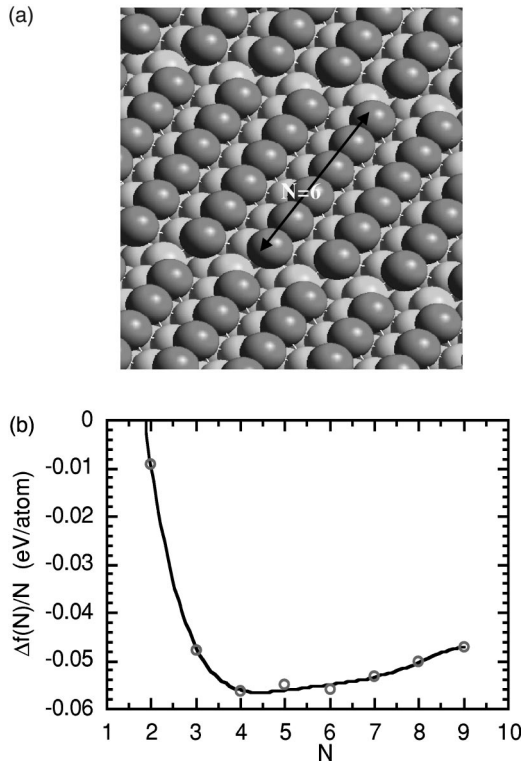

FIG. 2. Stress release with periodic vacancies in the Pd overlayer: (a) surface view for 6 Pd atoms on 7 Ni substrate atoms; (b) energy (eV per Pd atom) vs the number of Pd atoms N between vacancies. The energy reference is the epitaxial monolayer deposit.

ing periodically one Pd atom from the adlayer, in the $[1\bar{1}0]$ direction. So, N atoms remain in the adlayer and the periodicity of the structure in the $[1\bar{1}0]$ direction corresponds to $(N+1)$ Ni atoms in the substrate. The structure had been called $N/(N+1)$, with N varying between 2 and 9. Figure 2(a) shows the vacancy obtained in a 6/7 structure.

Concerning the stability of these structures, the main results are recalled below. The adsorption energies of the $N/(N+1)$ structures are presented in Fig. 2(b), as a function of the number N of Pd atoms. This curve presents a minimum around $N=4-6$ corresponding to an average Pd adsorption energy of 56 meV/atom. The shape of this curve was discussed as coming from a competition between three main contributions:[9] the vacancy creation energy that results from a Pd-Pd bond breaking, the stress release energy that comes from the fact that the Pd-Pd distances relax and increase as compared to the epitaxial situation, and, finally, the epitaxial contribution due to the displacement of the Pd out of their Ni-epitaxial sites.

In the [001] direction, there is a correlation between the Pd rows that could explain why, at low coverage, ordered periodical structures are observed by STM. For a 7×2 cell, with a vacancy in each of its two $[1\bar{1}0]$ rows, we have calculated the energy as a function of the number of sites separating the two vacancies. Figure 3(a) illustrates a case with two in-phase vacancies (rows A and B), and a case with a separation of two sites between the vacancies (rows B and C). The energy [Fig. 3(b)] is minimum when the vacancies

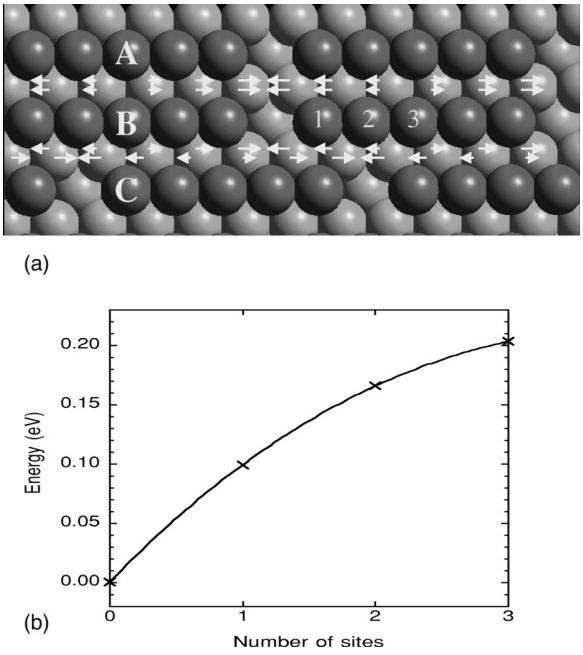

FIG. 3. Registry of vacancies in the direction perpendicular to the rows: (a) surface view of an example of possible separations between vacancies on adjacent rows; the arrows indicated the in-phase (favorable) or out-of-phase (unfavorable) relaxation of the substrate Ni atoms; (b) surface energy (eV) vs number of sites between vacancies.

are in-phase and increases strongly with the vacancies separation: the energy increase is about 200 meV for a distance of three sites between the vacancies, compared to the in-phase situation (0 sites). This effect explains why all the vacancies tend to be in-phase, therefore inducing a $N\times1$ reconstruction. This curve can be explained by taking into account the underlayer Ni substrate. The Pd atoms at the end of the Pd island exert forces on the underlying Ni atoms so that they move in the direction that reduces the cost of the epitaxial energy. When the vacancies are in-phase, the Ni atoms which are shared by the two rows are pushed in the same direction, as shown in the case of the Ni underlayer between rows A and B [see white arrows in Fig. 3(a)]. In contrast, as illustrated by the white arrows between rows B and C, the two sets of forces coming from the B row, and from the C row are shifted and on most of the Ni atoms the forces have opposite directions. So, when the vacancies are out of phase, the underlying Ni atoms are pushed in opposite directions and cannot move. This local stress increases the energy. So, the peculiar reconstruction of this family of $N/(N+1)$ structures appears to be driven by the relaxation of stress, both in the $[1\bar{1}0]$ and the [001] directions.

4. Reaching the 1 monolayer structure

Within this stress release mechanism by vacancy formation, the coverage is always lower than one. It is, however, possible to reach the monolayer in a similar reconstruction if on a $N/(N+1)$ structure, one additional Pd atom is added covering a site between two adjacent vacancies [Fig. 4(a)]. This adatom looks like the starting point of a second layer

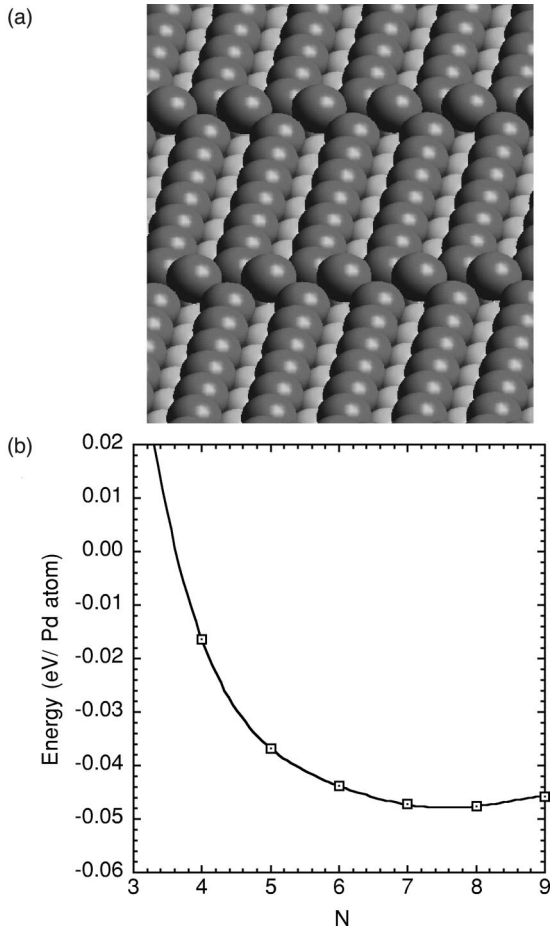

FIG. 4. 1 ML coverage: stress release by formation of a defect in the Pd overlayer: (a) surface view; (b) energy (eV per Pd atom) as a function of the number of Pd atoms separating the defects. The energy reference is the epitaxial monolayer deposit.

over a defective first layer. This set of periodical structures is called $(N+1)(d)/(N+1)$, where $(N+1)$ corresponds to the number of Ni epitaxial sites by unit cell as well as the number of deposited Pd atoms, making up a defect (d) monolayer.

For this $(N+1)(d)/(N+1)$ family, the energy curve, versus N, is depicted in Fig. 4(b). It presents the same shape as the $N/(N+1)$ structure energy behavior [Fig. 2(b)], the main feature being a shift in the minimum position. The optimum period is around $N=8$, with an energy of -48 meV by Pd atom. Therefore, in these $(N+1)(d)/(N+1)$ structures, the Pd atoms appear to be nearly as stable as the $N/(N+1)$ structure, despite the Pd atom on top of the vacancies. What is the energy contribution of this peculiar adatom? The computation of the adsorption energy of one Pd on a $N/(N+1)$ structure, giving a $(N+1)(d)/(N+1)$ structure, is presented in Fig. 5. The adsorption energy becomes more and more favorable as N increases. This behavior can be related to the vacancy size of the underlaying $N/(N+1)$ structure. As N increases the vacancy length is decreasing, and the adsorption of the adatom becomes more stable, by optimizing the Pd-Pd and Pd-Ni bond distance. The balance between this adsorption energy and the energy behavior of the $N/(N+1)$ structure versus N induces an increase of the optimal cell period. We can conclude that the $(N+1)(d)/(N+1)$ structures are stable, since they keep much of the stress release of the $N/(N+1)$ Pd islands, while the Pd adatom brings a compensation to the bond loss associated to the vacancy formation.

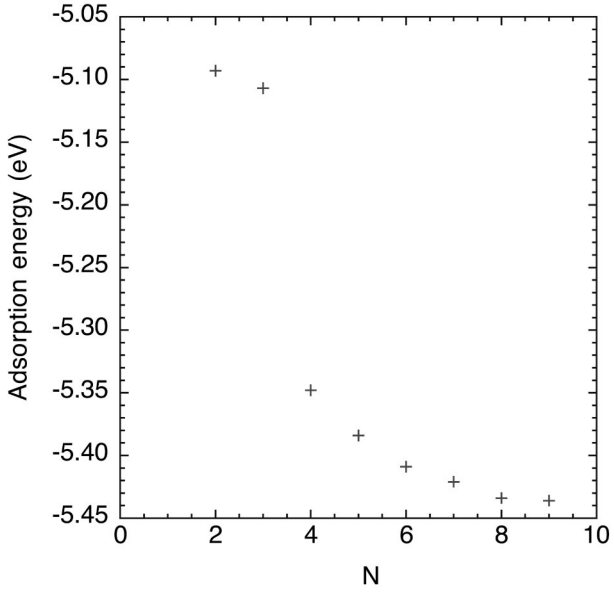

FIG. 5. From the vacancy to the defect structure: adsorption energy (eV) of a Pd atom on a $N/(N+1)$ structure, vs N.

This $(N+1)(d)/(N+1)$ family is intrinsically less stable than the $N/(N+1)$ structure, but it can accomodate more Pd by unit cell than the $N/(N+1)$. Its absolute stability will be discussed in the phase diagram section.

B. High-coverage structures

In order to hint for surfaces that are experimentally more active for catalysis, we have studied other families of structures at higher coverages (2–4 monolayers).

1. 2 monolayer structure

The more obvious way to get a stable higher-coverage structure is to start from the $(N+1)(d)/(N+1)$ structure and build up a second layer of N Pd including the adatom previously mentioned. This family has a coverage close to 2 ML [$2N/(N+1)$, where $N+1$ is the number of Ni sites] and is illustrated in Fig. 6(a), in the case of $N=6$. The optimization of the structure shows that the second Pd layer presents a periodical undulation, but without any vacancy. This kind of structure can be seen as a starting corner dislocation that allows the transition between the underlayer of $(N+1)$ Ni atoms and the surface layer of N Pd atoms. Dislocations on heteroepitaxial deposits have been observed in many systems.[23–26] The top Pd atoms are then close to their optimal parameter (2.75 Å) and the stress can be considered as mainly released from the creation of this array of dislocations. The energy behavior of this 2 ML family, versus the number N of surface Pd, has still the same shape as in the two previous structures [Fig. 6(b)]. The energy by Pd atom

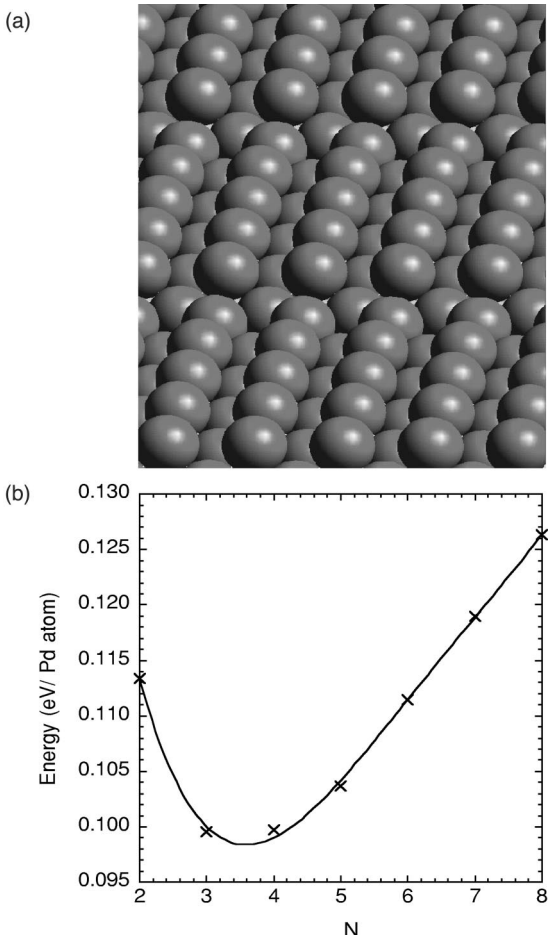

FIG. 6. 2 ML deposit structure with vacancies in the first layer: (a) surface view; (b) energy vs N (number of Pd atoms in the first layer separating the vacancies). The energy reference is the epitaxial monolayer deposit.

curve presents a minimum for N around 4. With our energy reference, the minimun energy is 0.1 eV less stable than the purely epitaxial surface at 1 ML coverage. Then, the adsorption energy is weaker than that of the Pd monolayer. We have also tried to find a $\Lambda\times 2$ reconstruction for this coverage, but none was found to be stable.

2. 4 monolayer structures

The optimal catalytic activity is obtained for deposits around 4 ML. Therefore, we studied structures that come from the growth of the previous 2 ML structure, just by filling two more layers. The final coverage corresponds to 4N Pd atoms over $N+1$ Ni sites, with the dislocative vacancy in the first layer [Fig. 7(a)]. Experimentally,[7,8] the surface was found to be reconstructed in a $\Lambda\times 2$ way ($\Lambda=9$–10). So, in order to investigate this behavior, we have computed $(N+1)\times 2$ cells, but, because of the large size of the cell, the calculation of all the members of this family was not possible: the 11×2 structure needs an unit cell with 190 atoms and 1900 electrons, which is very large in terms of computing time. Therefore, we have only studied the 7×2 (Fig. 7), 11×2 (Fig. 8), and the 1×2 epitaxial 4 ML surfaces. The

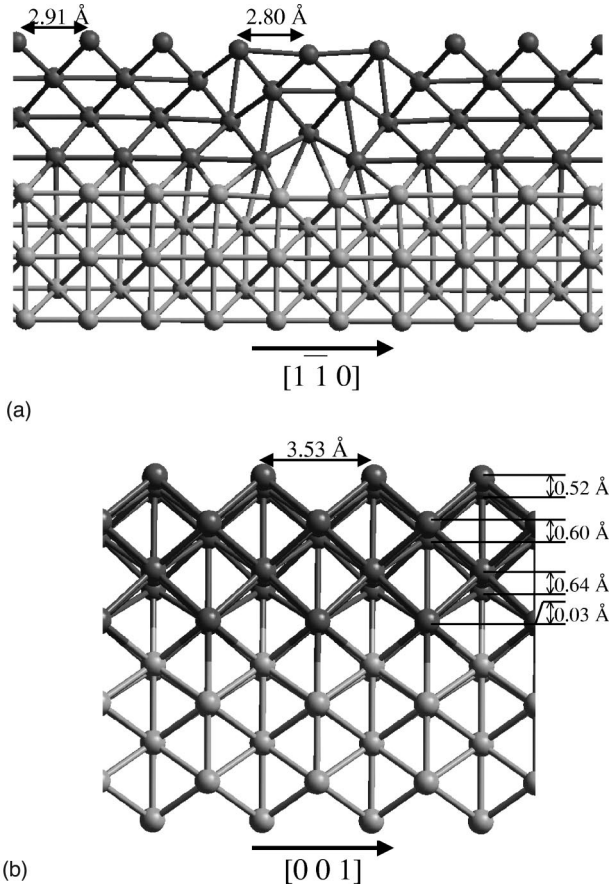

FIG. 7. 4 ML deposit structure with an array of corner dislocations at the interface: 7×1 reconstruction: (a) view along the $[1\bar{1}0]$ direction (5 Ni substrate layers are shown in light balls); (b) view along the [001] direction: no pairing present.

7×2 structure converges to an island aggregation in the $[1\bar{1}0]$ direction [Fig. 7(a)], with no pairing in the [001] direction and a geometry converging toward a 7×1 structure [Fig. 7(b)]. In the vicinity of the vacancy, there is a large buckling in the the Pd second layer, and the influence of the dislocation propagates up to the surface layer. With this short separation between dislocations, the resulting Pd-Pd distance is large (up to 2.91 Å) and the initial compressive stress in the epitaxial system is overcompensated.

The 11×2 structure is much more ordered and shows two kinds of perpendicular reconstructions. The first one, in the $[1\bar{1}0]$ direction [Fig. 8(a)], can again be seen as a dislocation. Compared to the previous structure, the dislocation is much more localized at the interface and the ordered structure more or less recovered already in the second Pd layer, in the $[1\bar{1}0]$ direction. The Pd-Pd distance along the row at the surface ranges between 2.73 and 2.75 Å, close to the optimal Pd diameter at surface.[9] This structure shows a second reconstruction, in the [001] direction [Fig. 8(b)], which has a pairing and buckling structure. Such a pairing reconstruction was shown to be unstable for a pure Pd(110) surface[27] and is specific of these deposits on Ni(110). At the surface new Pd-Pd bonds are formed between adjacent rows, while the distance between Pd neighbors in the first and third layer is

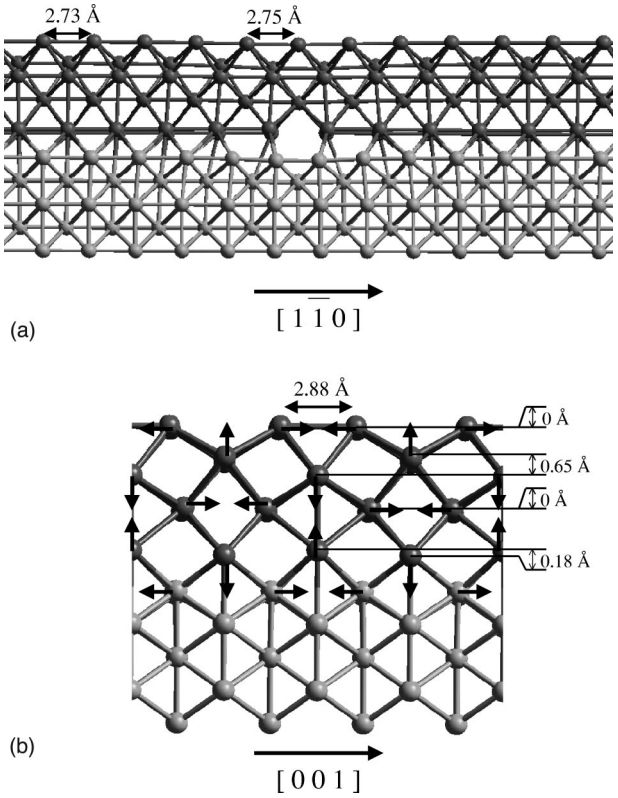

FIG. 8. 4 ML deposit structure with an array of corner dislocations at the interface: 11×2 reconstruction: (a) view along the $[1\bar{1}0]$ direction; (b) view along the [001] direction. Displacements for the pairing reconstruction are indicated by arrows.

increased. Moreover, the detailed structure and behavior of these surfaces was compared, with very good agreement, to experimental results.[28]

IV. PHASE STABILITY DIAGRAM

In the previous section, we have shown that many locally stable structures can exist for the Pd/Ni(110) surfaces. The question that needs now to be clarified is to classify the stability of all structures and to extract some phase stability diagram as a function of the Pd coverage.

A. Comparison between structures

In order to built the phase stability diagram we define

$$\tau=\frac{N}{S} \tag{1}$$

where τ is the mean coverage of a total of N Pd atoms deposited on S epitaxial site of a Ni surface. If two different structures 1 and 2 coexist at the surface, the local coverage, τ_1 and τ_2 are defined by

$$\tau_i=\frac{N_i}{S_i} \quad (i=1,2) \tag{2}$$

where N_i and S_i are, respectively, the number of Pd atoms and of epitaxial sites in the unit cell of the considered structure i. If n_1 and n_2 are the number of unit cells of the structures 1 and 2, respectively, we get the following equations, from the conservation of the Pd atoms and of the number of epitaxial sites:

$$n_1=\frac{N_2S-S_2N}{S_1N_2-S_2N_1} \tag{3}$$

and analogously for n_2.

So, when a surface with a mean Pd coverage of τ dissociates into two phases formed by structures 1 and 2 that have a coverage rate τ_1 and τ_2 and a Pd adsorption energy E_1 and E_2 respectively, the average adsorption energy $\overline{E}$ of Pd atoms on this the surface is given by

$$\tau\overline{E}=\frac{\tau-\tau_2}{\tau_1-\tau_2}\tau_1E_1+\frac{\tau-\tau_1}{\tau_2-\tau_1}\tau_2E_2. \tag{4}$$

Therefore, the relevant energy variable appears to be τE for describing the phase stability diagram. This is the average adsorption energy of Pd atoms by Pd atom and by Ni site and the most stable surface minimizes this energy.

This relation can be modified using an homomorphic transformation. Let us define the reduced coverage

$$\tau_i'=\frac{\tau_i}{1+\tau_i}. \tag{5}$$

Then, we get

$$\tau'\overline{E}=\frac{\tau'-\tau_2'}{\tau_1'-\tau_2'}\tau_1'E_1+\frac{\tau'-\tau_1'}{\tau_2'-\tau_1'}\tau_2'E_2. \tag{6}$$

This transformation induces a change of scale: as the coverage τ is varying between 0 and ∞, the reduced coverage τ' has a range between 0 and 1.

Then, we express the reduced energy $\tau'\overline{E}$ of all our structure versus their reduced coverage τ'. In this representation, the stable structures are associated with the convex envelope of the whole set of curves. When the curve of a family constitutes the convex envelope, it means that these structures are stable. In contrast, when the convex envelope is created from a straight line between two structures, the surface composition is a mixing of these two structures. In that case, the lever rule gives the proportion of the two structures by the relative position of the total reduced coverage on the line.

B. Entropy

To get the proper phase stability diagram at temperatures over 0 K, we have to take into account the entropy as part of the free energy. But, for condensed matter, entropy is always quite difficult to extract completely from calculations. So, in this article, we just consider the mixing entropy: since the surfaces presented are analogous, with Pd deposited on the same substrate of Ni, the vibrational entropy is expected to behave similarly for all them and can be neglected for comparisons.

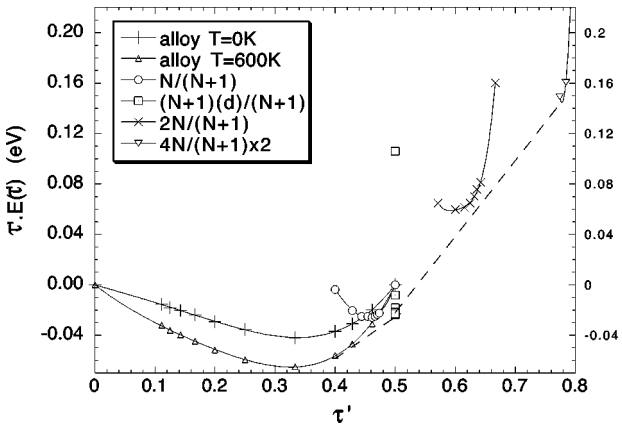

FIG. 9. Phase stability diagram showing the reduced energy $\tau' E(\tau')$ (eV) vs the reduced coverage τ' (see text for definition) for several families of deposit structures: surface alloys with (up triangles) and without (plus) mixing entropy contribution, vacancy structure (circles), defect structure (squares), 2 ML (crosses), and 4 ML (down triangles) structures with an array of dislocations at the interface. The dashed line forms the convex envelope of these energy curves. The energy reference is the epitaxial monolayer deposit.

The mixing entropy is large for the alloy phase, that we consider to be unordered. To express this entropy (by Pd atom) we use the classical canonical expression for alloys:

$$\Delta S = k_B \frac{\tau'-1}{\tau'}\left[\frac{\tau'}{1-\tau'}\ln\left(\frac{\tau'}{1-\tau'}\right)+\frac{1-2\tau'}{1-\tau'}\ln\left(\frac{1-2\tau'}{1-\tau'}\right)\right], \tag{7}$$

where ΔS is the mixing entropy by Pd atom on the surface and k_B the Boltzmann constant. We transform this expression to get the reduced entropy:

$$\tau'\Delta S = k_B[(1-\tau')\ln(1-\tau')-\tau'\ln(\tau')-(1-2\tau') \times \ln(1-2\tau')], \tag{8}$$

where $\tau'\Delta S$ is the reduced mixing entropy by the Pd atom and τ' is the reduced coverage. All the other structures we have studied in this article are highly ordered, so their mixing entropy is considered as negligible.

C. Stability of these structures

Figure 9 presents the phase stability diagram for the deposits of Pd on Ni(110) surfaces, showing the reduced energy as a function of the reduced coverage. At low coverage, the stable structures are the alloy surfaces. At 600 K, this structure is stable between $\tau'=0-0.4$, and even at 0 K, without the stabilization due to the mixing entropy, it appears to be stable as far as $\tau'=0.38$. Between $\tau'=0.4$ and 0.5, the stability curve is a convex envelope, which means that the surface is formed by the coexistence of two phases: the surface alloy, with a composition $\tau'=0.4$, and the 1 ML structure ($\tau'=0.5$), described in Sec. III A 4, the most stable within this family being the $8(d)/8$ surface. The vacancy structure, $N/(N+1)$, appears to be unstable: it dissociates into the $8(d)/8$ structure and the alloy surface of composition $\tau'=0.4$. At τ' above 0.5, the phase stability diagram presents another envelope between the 8(d)/8 structure and a 4 ML surface. From a quadratic fit with the calculated 7×2, 11×2, and 1×2 structures, the most stable 4 ML structures can be assigned to 9×2 or 10×2 surfaces, which correspond respectively to τ' around 0.78. So, the surface should present a mixing between the 1 ML and 4 ML structures. Between these two limit structures, the phase stability diagram shows that the 2 ML surface is less stable than the mixing. Nevertheless, some other possibilities could be investigated: for example, the structures around 3 ML ($\tau'=0.75$) might happen to be stable and then induce other mixing lines. However, the shape of our phase stability diagram should not be strongly modified.

To summarize, in this phase stability diagram, three kinds of stable structures appear: the family of surface alloys, up to $\tau'=0.4$, the 1 ML defect structure $[8(d)/8]$ and the 4 ML structure, with a 9×2 or 10×2 reconstruction. It must be emphasized that these stable structures are not necessarily those that have the strongest Pd atomic adsorption energy, since the total energy of the surface per unit area takes into account the number of Pd atoms on the surface. For instance, the alloy surface at $\tau'>0.4$ still has a Pd adsorption energy larger than that of the 1 ML structure, but a better energy compromise is found by disproportionating in the $\tau'=0.4$ and the 1 ML, $\tau'=0.5$ structures. Theses two limits allow the minimization of the average energy by Ni surface area. Similarly, the adsorption energy of the Pd atoms on the $N/(N+1)$ structure is larger [Fig. 2(b)] than that of the Pd atoms on the $8(d)/8$, 1 ML, surface. But, the latter can accommodate more Pd atoms than the former, for the same Ni surface area, then, it minimizes the total energy of the surface.

V. DISCUSSION: VARIATION OF ELECTRONIC PROPERTIES

As shown in the previous section, the deposits of Pd on Ni(110) surfaces present a large diversity of structures as a function of the coverage. Surface phase transitions occur, changing the composition and the geometrical aspect of the top layer of Pd atoms. Can we relate these structural variations with the catalytic activity and selectivity of the surface? Actually, this investigation needs a specific study of the adsorption and reactivity phenomena induced by these peculiar surfaces. Nevertheless, assuming, as is usually done, that the adsorption and the reactivity are mainly related to the electronic structure of the metal surface, it is important to understand the electronic features of the surface structures that we have emphasized from our phase stability analysis. This can be done by using the local density of states (LDOS) associated with the various Pd atoms of the considered surfaces. A descriptor of the chemisorption properties that was used previously[29–31] is the center of the *d* band of the LDOS of the surface atoms. There, we will present two parameters: the *d*-electron energy average on the occupied states η_1 (very close in practice to the center of the *d* band), and the width of the occupied *d* band, η_2. These two parameters are usually

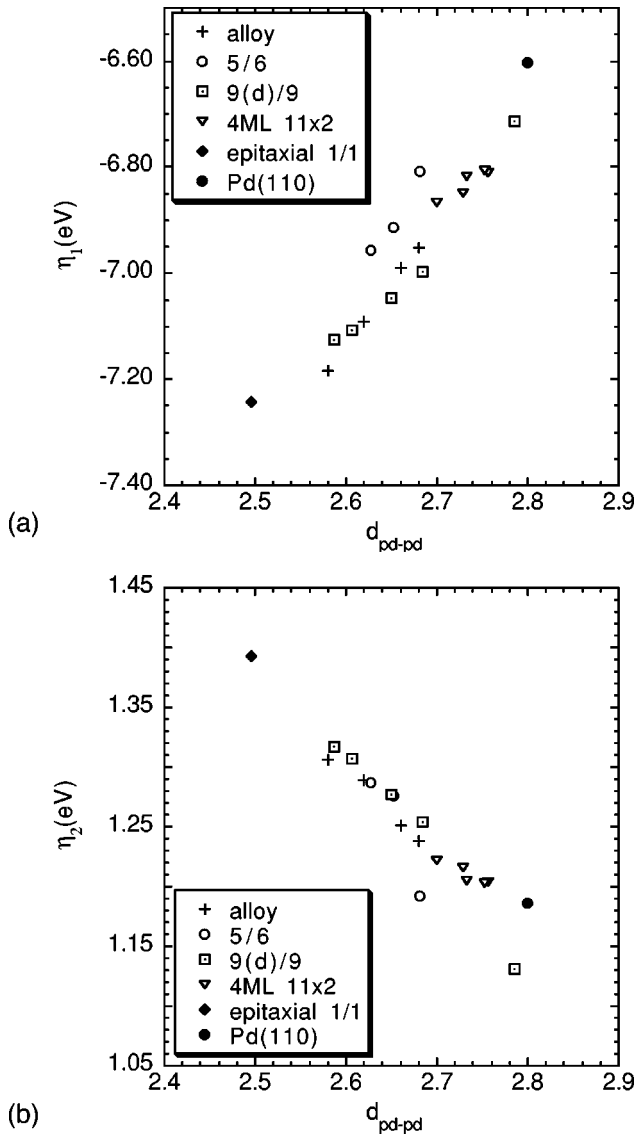

FIG. 10. Electronic properties of the surfaces projected on a surface Pd atom: (a) *d*-band center energy η_1 (eV) vs average Pd-Pd distance; (b) *d*-band width η_2 vs average Pd-Pd distance. Structures are pure Pd(110) (black diamond), epitaxic 1 ML deposit (black circle), surface alloys (plus), 5/6 vacancy structure (circle), 9(*d*)/9 defect structure (square), 4 ML array of dislocations with 11×2 reconstruction (down triangle).

correlated: a more narrow *d* band with identical *d* band center would have more states below the Fermi level, for metals on the right of the periodic table, such as Pd or Ni. This would result in a charge transfer toward the *d* states. Self-consistent field effect will prevent this charging, and the *d* states will shift up in energy in order to give a quasi-charge-neutrality. Hence narrow bands will have a higher *d*-band center energy compared to wide bands. Three aspects of the surface structure can be analyzed through η_1 and η_2: the effect of surface stress, the influence of surface alloying, and the role of the $\Lambda\times2$ pairing reconstruction. The computed values of η_1 and η_2 are given in Fig. 10, as a function of the surface Pd-Pd distance, calculated as the average distance between the considered Pd atom for the projection and all its surface Pd neighbors, in the considered structure. All nonequivalent Pd atoms are indicated for each structure. This average distance is related to the compressive stress ''felt'' by the Pd atom in the deposit: a short distance (2.49 Å) for a large compressive stress on the epitaxic structure, and a largest distance when the stress is released, as in reconstructed structures with vacancies and defects. The largest Pd-Pd distance (2.80 Å) corresponds to the pure Pd(110) surface. A linear correlation appears between this local atomic Pd-Pd distance and the change in the electronic properties, η_1 and η_2. This behavior has already been theoretically predicted in many homogeneous surfaces under stress,[11,12,14] and it is extended here to surfaces presenting Pd with different residual stress and local distance environment. The correlation previously described between the *d*-band center and the *d*-band width is clearly visible by comparing Figs. 10(a) and 10(b). The strongest effect of the stress can be observed directly on the epitaxial 1/1 structure, corresponding to the parameter of the Ni sublayer, 2.496 Å. It presents a large decrease of the mean energy, $\eta_1=-6.60$ eV, and a marked increase of the width, $\eta_2=1.19$ eV, as compared to the pure Pd(110) surface with the 2.80 Å parameter ($\eta_2=1.38$ eV, and $\eta_1=-7.24$ eV. The shorter Pd-Pd distance increases the coupling between Pd *d* states on the surface, and hence the *d* band is wider than that of the pure Pd surface. Being wider, the *d*-band center is lower in energy, in order to prevent a loss of electronic population on the Pd atoms. In the vacancy structure, $N/(N+1)$, and the 1 ML, $(N+1)(d)/(N+1)$, structures, the effect depends on the Pd environment since the local stress is not homogeneous. The surface Pd atoms yield a wide set of average distances between one given Pd and its neighbors. So, the electronic properties of these surfaces are finely tuned by the selected Pd atom position and residual stress. This can be seen in Figs. 10(a) and 10(b) in the case of the η_1 and η_2 electronic properties for the various surface Pd atoms of the vacancy 5/6 and the defective 9(*d*)/9 structures. The main effect of the increase of the stress on the Pd atoms is to decrease the local *d*-band average energy η_1 and to increase the *d*-band dispersion width η_2. The alloy Pd surfaces presents the same electronic behavior as a compressed Pd structure. For the 0.5 ML, with the Pd-Pd-Ni-Ni surface unit cell, the positions of the η_1 and η_2 are in agreement with the Pd-Pd distance of 2.66 Å. This confirms the compressive stress to which Pd atoms are submitted, as we have assumed to explain the energy behavior of the alloy surface. As the alloy dilution increases, an increase of η_1 and a decrease of η_2 are observed. This is fully consistent with a stress decrease.

The four layer 11×2 surface has a different geometry since it shows a pairing reconstruction in the (100) direction. However, this reconstruction seems to have little influence on the average electronic properties of the surface atoms, since the 11×2 surface follows the same linear correlation as the other structures. Two electronic structures clearly depart from the linear correlation, especially with a reduced bandwidth η_2. These correspond to atoms with smaller metallic coordinations: the Pd atom next to the vacancy in the 5/6 system and the one capping the defect for 9(*d*)/9.

We conclude that the stress on the surface Pd atoms has

large consequences on the electronic properties, with a wider and lower projected *d*-band DOS for locally compressed atoms. Of course, this behavior can strongly influence the reactivity of molecules adsorbed on these surfaces. One point that appears here is that the ideal structure of purely epitaxial Pd/Ni(110) is subject to a strong stress and hence its electronic structure is far away from that of more stable surfaces which have been extracted from the phase diagram, and where a large part of the compressive stress is released by formation of arrays of dislocations. So, model epitaxial surfaces seems to be quite far from more realistic ones, and are expected to behave differently. To explain more precisely the surface reactivity of these kind of bimetallic compounds, it might be important to take into account the electronic properties of the realistic stress released stable structures. Surprisingly, the four-layer deposit, which gives the largest activity, is the one with the smallest strain in the surface Pd atoms, compared to pure Pd. It shows the weakest increase in *d*-band width, and the smallest *d*-band center down-shift compared to Pd. This could put some doubts on the relation between strain and reactivity in this case, although the observed *d*-band shift is still around 0.25 eV. Three hypothesis can be put forward in order to explain this increase of reactivity. First, the electronic structure needs to be analyzed since specific orbitals as dz^2 can have a crucial influence in the interaction with molecules. Then, it could also be explained by the presence of defects that could be especially reactive, as shown by recent calculations.[32] Moreover, upon adsorption, but also during the activation step, important structural changes could appear on the surface and thus the reactivity behavior of these surfaces cannot be simply extracted from these crude variations of electronic structure. The reactivity of this 4 M.L. deposit for the hydrogenation of ethylene is under investigation.

VI. CONCLUSION

In this paper, we have studied several families of deposits of Pd on Ni(110) surfaces, from low coverage, with disordered alloyed and vacancy defect structure, to higher 4 ML coverage, with an 11×2 reconstruction. The competition between the stress and the epitaxy seems to drive the observed reconstructions, yielding a wide range of dislocative structures. In the alloy case, the stress is opposed to the alloying, and as the coverage increases, the stress is becoming so strong above 0.67 ML that this induces a demixing of the alloy. The calculations show microscopic structures for corner dislocations: at 1 ML, the dislocation is reduced to a simple vacancy with a Pd atom on top. The stress in the $[1\bar{1}0]$ direction is efficiently released, but there is still some residual stress in the [001] direction. This stress increases with the coverage and finally induces some $\Lambda\times2$ reconstructions that are not stable for the pure Pd(110) surface. These structures present very peculiar surface coordinations with nearly square surface sites and important subsurface buckling and pairing reconstruction. They are expected to have particular behavior for many catalytic reactions. Another aspect associated with the complexity of these structures is the dispersion of the local stress. This is associated with an important change in the electronic properties, with the variation of the projected *d*-band center η_1 by 0.5 eV and *d*-band width η_2 by 0.2 eV. The control of the deposit coverage could be an useful way to tune the electronic properties of a surface and to design optimized catalytic surfaces for a chosen reaction.

The next step is then to understand the link between the surface structure and electronic properties, and the reactivity of molecules on these surfaces. For that purpose, studies of the reactivity on these surfaces and their link to the surface structure are under investigation.

ACKNOWLEDGMENTS

This work has been performed within the Groupement de Recherche Européen ''Dynamique Moléculaire Quantique Appliquée à la Catalyse,'' a joint project of the Conseil National de la Recherche Scientifique (CNRS), Institut Français du Pétrole (IFP), TOTALFINA, Universität Wien, and Schuit Institute of Catalysis. It was also supported by the ''Région Rhône-Alpes'' under Contract No. 7000 66 14 and by the computational resource center IDRIS (CNRS) under Contract No. 00609.

[1] F. Besenbacher, L. Pleth Nielsen, and P. T. Sprunger, *The Chemical Physics of Solid Surfaces*, edited by D. A. King and D. P. Woodruff (Elsevier, Amsterdam, 1997), Vol. 8.
[2] P. Hermann, B. Tardy, D. Simon, and J.-C. Bertolini, Surf. Sci. **307-309**, 422 (1994).
[3] P. Hermann, B. Tardy, Y. Jugney, D. Simon, and J.-C. Bertolini, Catal. Lett. **36**, 9 (1996).
[4] P. Hermann, J.-M. Guigner, B. Tardy, Y. Jugney, D. Simon, and J.-C. Bertolini, J. Catal. **163**, 169 (1996).
[5] J.-C. Bertolini, Surf. Rev. Lett. **3**, 1857 (1996).
[6] J.-C. Bertolini, Appl. Catal., A **191**, 15 (2000).
[7] L. Porte, M. Phaner-Goutorbe, J. Guigner, and J.-C. Bertolini, Surf. Sci. **424**, 262 (1999).
[8] M. Abel, Y. Robach, J.-C. Bertolini, and L. Porte, Surf. Sci. **1**, 454 (2000).
[9] J.-S. Filhol, D. Simon, and P. Sautet, Surf. Sci. **472**, L139 (2001).
[10] J.-M. Roussel, A. Saúl, and G. Tréglia, Phys. Rev. B **55**, 10 931 (1997).
[11] *Stress and Strain in epitaxy: Theoretical Concepts, Measurements and Applications*, edited by Margrit Hanbücken and Jean Paul Deville (North-Holland, Amsterdam, 2001).
[12] *Advances in Catalysis*, edited by Bruce C. Gates and Helmut Knozinger (Academic, San Diego, 2000).
[13] J. A. Rodriguez, Heterog. Chem. Rev. **3**, 17 (1996).
[14] M. Mavrikakis, B. Hammer, and J. K. Nørskov, Phys. Rev. Lett. **81**, 2819 (1998).
[15] V. Pallassana and M. Neurock, J. Catal. **191**, 301 (2000).
[16] G. Kresse and J. Hafner, Phys. Rev. B **49**, 14 251 (1994).
[17] G. Kresse and J. Furthmüller, Comput. Mater. Sci. **6**, 15 (1996).

[18] D. Vanderbilt, Phys. Rev. B **41**, 7892 (1990).
[19] G. Kresse and J. Hafner, J. Phys.: Condens. Matter **6**, 8245 (1994).
[20] J. P. Perdew, J. A. Chevary, S. H. Vosko, K. A. Jackson, and M. R. Pederson, Phys. Rev. B **46**, 6671 (1992).
[21] P. J. Feibelman, Phys. Rev. B **51**, 17 867 (1995).
[22] P. J. Feibelman, Phys. Rev. B **56**, 2175 (1997).
[23] J. Hamilton and S. Foiles, Phys. Rev. Lett. **75**, 882 (1995).
[24] H. Ibach, Surf. Sci. Rep. **29**, 193 (1997).
[25] H. Brune, M. Giovannini, K. Bromann, and K. Kern, Nature (London) **394**, 451 (1998).
[26] I. Meunier, G. Tréglia, J.-M. Gay, B. Aufray, and B. Legrand, Phys. Rev. B **59**, 10 910 (1999).
[27] V. Ledentu, W. Dong, P. Sautet, G. Kresse, and J. Hafner, Phys. Rev. B **57**, 12 482 (1998).
[28] J.-S. Filhol, M.-C. Saint-Lager, D. Simon, and P. Sautet (unpublished).
[29] A. Ruban, B. Hammer, P. Stolze, H. L. Skriver, and J. K. Nørskov, J. Mol. Catal. A: Chem. **115**, 421 (1997).
[30] V. Pallassana, M. Neurock, L. B. Hansen, B. Hammer, and J. K. Nørskov, Phys. Rev. B **60**, 6146 (1999).
[31] V. Pallassana, M. Neurock, L. B. Hansen, and J. K. Nørskov, J. Chem. Phys. **112**, 5435 (2000).
[32] B. Hammer, Phys. Rev. Lett. **83**, 3681 (1999).